J Therm Anal Calorim (2014) 115:2429–2437
DOI 10.1007/s10973-013-3367-x

Inclusion complex of (−)-linalool and β-cyclodextrin

P. P. Menezes · M. R. Serafini · L. J. Quintans-Júnior · G. F. Silva · J. F. Oliveira · F. M. S. Carvalho · J. C. C. Souza · J. R. Matos · P. B. Alves · I. L. Matos · Daniel I. Hădărugă · A. A. S. Araújo

Received: 5 May 2013 / Accepted: 2 August 2013 / Published online: 1 September 2013

Abstract (−)-Linalool is a monoterpene alcohol which is present in the essential oils of several aromatic plants. Recent studies suggest that (−)-linalool has antimicrobial, anti-inflammatory, anticancer, antioxidant, and antinociceptive properties in different animal models. The aim of this study was to prepare and characterize inclusion complexes of (−)-linalool with β-cyclodextrin (β-CD). Equimolar binary (−)-linalool/β-CD systems were prepared by physical mixture, paste (PM), and slurry methods (SC) and characterized by differential scanning calorimetry, thermogravimetric analysis, FT-IR spectroscopy, X-ray diffractometry, Karl Fisher titration, and scanning electron microscopy. Thermal characterization indicates the occurrence of complexation, mainly in paste complexes, which is present in the interval from 140 to 280 °C a gradual mass loss (4.6 %), probably related to (−)-linalool loss. FT-IR spectra showed changes that may be related to the formation of intermolecular hydrogen bonds between (−)-linalool and β-CD. The new solid-phase formed using the PM and SC methods, had a crystal structure which was different from the original morphology of β-CD.

Keywords (−)-Linalool · Monoterpene · Inclusion complexes · Cyclodextrins

Introduction

(−)-Linalool (Fig. 1) is a naturally occurring enantiomer monoterpene alcohol compound prevalent in essential oils of various aromatic plant species [1]. It may be found in fragrances used in decorative cosmetics, fine fragrances, shampoos, toilet soaps, and other toiletries as well as in non-cosmetic products. As well, linalool was approved by the Food and Drug Administration (FDA) as GRAS ('generally recognized as safe'), substances used as spices and food additives [2]. This monoterpene is also the principal component of many essential oils known to exhibit several biologic activities such as antibacterial, antiinflammatory, antihyperalgesic, antinociceptive, and antiplasmodial effects [1, 3–5].

Several complexation methods have been reported to applications in the drug, cosmetics and food industry, as a flavor carrier and as a treatment to impart some degree of

P. P. Menezes · M. R. Serafini · L. J. Quintans-Júnior · J. C. C. Souza · A. A. S. Araújo (✉)
Departamento de Fisiologia, Universidade Federal de Sergipe, Av. Marechal Rondon, s/n, Cidade Universitária, São Cristóvão, Sergipe 49100-000, Brazil
e-mail: adriasa2001@yahoo.com.br

G. F. Silva
Departamento de Engenharia Química, Universidade Federal de Sergipe, Av. Marechal Rondon, s/n, Cidade Universitária, São Cristóvão, Sergipe 49100-000, Brazil

J. F. Oliveira · J. R. Matos
Departamento de Química Fundamental, Instituto de Química, Universidade de São Paulo, Av. Lineu Prestes, 748, São Paulo, SP 05508-000, Brazil

F. M. S. Carvalho
Departamento de Mineralogia e Geotectônia, Instituto de Geociências, Universidade de São Paulo, São Paulo, SP, Brazil

P. B. Alves · I. L. Matos
Departamento de Química, Universidade Federal de Sergipe, Av. Marechal Rondon, s/n, Cidade Universitária, São Cristóvão, Sergipe 49100-000, Brazil

D. I. Hădărugă
Department of Applied Chemistry and Organic-Natural Compounds Engineering, Faculty of Industrial Chemistry and Environmental Engineering, "Politehnica" University of Timisoara, Victory Sq. 2, 300006 Timisoara, Romania

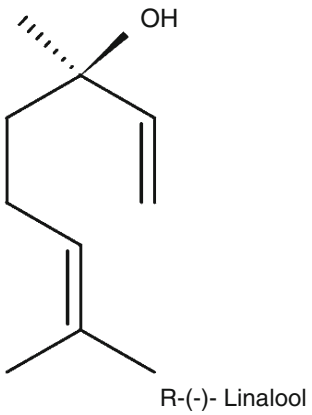

Fig. 1 Molecular structure of the linalool

protection against evaporation, oxidation, reaction or migration of active compounds [6–8]. Additionally, the complexes improve the characteristics of the drugs such as solubility, chemical stability, bioavailability, and reduction of drugs side effects [9–11].

Cyclodextrins (CDs) are water-soluble cyclic oligomers composed of 6–8 U of glucopyranose bonded together by α-(1,4) linkages. The most common form is β-CD, which is composed of 7 U of glucopyranose [10–14]. It has the shape of a hollow truncate cone. The hydrophilic outer surface and relatively hydrophobic inner cavity make it possible to form supramolecular inclusion complexes with many organic compounds [15, 16].

β-CD with linalool and camphor in *Lavandula angustifolia* essential oil was investigated by static headspace gas chromatography [17]. Ciobanu et al., reported that CDs reduce the volatility of the aroma compounds and stable 1:1 inclusion complexes are formed. The feasibility of preparation of novel-controlled release systems for the delivery of fragrances was investigated by multiple headspace extraction experiments.

The aim of the present work was to produce the β-CD inclusion complexes of (−)-linalool using physical mixture, slurry, and paste methods at stoichiometric ratio. Differential scanning calorimetry (DSC), infrared spectroscopy (FT-IR), thermogravimetry/derivative thermogravimetry (TG/DTG), scanning electron microscopy (SEM), and X-ray diffraction (XRD) were used to characterize the products.

Materials and methods

Material

(−)-Linalool or 3,7-dimethylocta-1,6-dien-3-ol (99,0 %) and β-cyclodextrin (98,0 %) were purchased from SIGMA (St. Louis, USA). All other chemical reagents were of at least reagent grade and all materials were used as supplied.

Preparation of inclusion complexes

Inclusion complexes were prepared by three different procedures. A physical mixture (PM) was prepared by the addition of (−)-linalool to an agate mortar containing powdered β-CD under manual agitation. The (−)-linalool/β-CD molar ratio was maintained as described for inclusion complex preparation and the mechanical mixture was stored in airtight glass containers. Paste complexation (PC) was carried out by homogenization of β-CD (1,135 mg) with water (1.2:4, w/v, mg/mL) directly in an agate mortar. In a second step, 154 mg of (−)-linalool (1:1 molar guest:host ratio) was added to β-CD paste under a constant manual agitation. Then, the material was dried at room temperature (in a desiccator) until a glass film was formed, which was removed by manual trituration and stored in airtight glass containers. Slurry complexation (SC) was carried out by the addition of water to a beaker containing 1,135 mg of β-CD (3:4, w/v, mg/mL). 154 mg of (−)-linalool, which is equal to about a 1:1 molar guest:host ratio, was added to the slurry and stirred for 36 h by a magnetic stirring device operating at 400 rpm (Quimis Q 261A21, Brazil). Thereafter, the mixture was transferred to an agate mortar, and dried in a desiccator.

Thermal analysis

DSC curves were obtained in a DSC-50 cell (Shimadzu) using aluminum crucibles with about 2 mg of samples, under dynamic nitrogen atmosphere (50 mL min^{-1}) and heating rate of 10 °C min^{-1} in the temperature range of 25–600 °C. The DSC cell was calibrated with indium (m.p. 156.6 °C; $\Delta H_{fus.} = 28.54$ J g^{-1}) and zinc (m.p. 419.6 °C). TG/DTG curves were obtained with a thermobalance model TGA 50 (Shimadzu) in the temperature range of 25–900 °C, using platinum crucibles with ~3 mg of samples, under dynamic nitrogen atmosphere (50 mL min^{-1}) and heating rate of 10 °C min^{-1}. Thermogravimetric system was calibrated using a $CaC_2O_4.H_2O$ standard substance in conformity to ASTM pattern [18].

Moisture determination

The moisture contents of the PM, slurry, and paste complexes were determined by the Karl Fisher method using a KF 1000 Analyzer (Brazil) and iodine solution, in the presence of pyridine (and sulfur dioxide) as titrating solution. The analyses were carried out in duplicate.

Fourier transform infrared spectroscopy (FT-IR)

The infrared absorption data were obtained in the range of 4,000−400 cm^{-1} in KBr pellets using an FT-IR Bomen spectrophotometer, model MB-120, at room temperature.

Scanning electron microscopy (SEM)

The dried products were mounted on copper tape and visualized with a JEOL Model JSM-7410-F scanning electron microscope, at an accelerated voltage of 1 kV.

X-ray diffractometry (XRD)

XRD patterns were obtained on a Siemens, model D5000, with tube of Cu Kα, in the interval of 3–65° (2θ) and 1 s of pass time, using the powder XRD method.

Gas chromatography/mass spectrometry (GC/GCMS) analyses

A multi-dimensional GC/GCMS system (QP2010 Ultra, Shimadzu Corporation, Kyoto, Japan) equipped with autoinjector AOC-20I (Shimadzu Corporation, Kyoto, Japan) was used for performing the analyses employing the following conditions: RestekRtx®-5MS fused silica capillary column (30 m × 0.25 mm i.d × 0.25 mm thickness film, composed of 5 %-diphenyl-95-dimethyl polissiloxane) was used. Helium (99.999 %) was used as carrier gas at a constant flow of 1.2 mL min^{-1} and an injection volume of 2.0 μL was employed (split ratio 1:10). The injector temperature 250 °C and the ion source temperature 200 °C. The oven temperature was programed to 60 °C with an increase of 3 °C min^{-1} to 230 °C.

The FID and MS data were acquired simultaneously using a detector separation system, the flow split ratio was 4:1 (MS: FID).Tube restrictor 0.62 m × 0.15 mm i.d (capillary column) was used to connect the splitter to the detector MS; tube restrictor 0.74 m × 0.22 mm i.d was used to connect the splitter to the detector FID. Mass spectra were taken at 70 eV, a scan interval of 0.3 s and fragments from 40 to 350 Da. FID temperature was adjusted to 250 °C, and the supplied gases to FID were synthetic air, hydrogen,and helium at flow rates of 30, 300, and 30 mL min^{-1}, respectively. Quantification of each constituent was estimated by normalizing the peak area generated in the FID—(%). Compounds concentrations were calculated from the GC peak areas and are arranged in order of elution from the GC.

Extraction of total linalool

(−)-Linalool adsorbed total in the β-CD was determined by extraction according to the method described by Marreto et al. Distilled water (8 mL) plus hexane (4 mL) and 0.2 g of the sample were put in a round bottom flask which was kept in a water-bath at 85 °C for 20 min, with constant shaking. The organic phase was decanted (3 times) and concentrated to approximately 1 mL using rotary evaporator. Then, internal padrão (2 mg) was added and stored until GC–MS/FID analysis.

Extraction of surface-adsorbed linalool

The amount of (−)-linalool adsorbed on the surface of β-CD was determined by washing. Sample (3 g) with hexane (20 mL) was shaken for 20 min. The suspension was filtered and the residue was washed with hexane (10 mL). Then, hexane (1 mL) and internal standard (2 mg) were added to the filtrate which was concentrated using rotary evaporator and analyzed by CG-EM/FID. Thus, the difference between the total linalool (surface-adsorbed linalool and hosted in the cavity) and the surface-adsorbed linalool corresponds to the amount complexed in the β-CD cavity.

Results and discussion

The formation of the (−)-linalool/β-CD inclusion complexes was studied by obtaining TG/DTG curves concerning pure (−)-linalool, β-CD alone, PM, PC, and SC. Figure 2 shows the TG curves of the materials and Table 1 lists the mass losses calculated from specific intervals for each material studied in the present work. By their data analysis, it can be seen that the major fraction of (−)-linalool decompose and volatilize up to 140 °C. β-CD, Fig. 2 shows thermoanalytical profile which can be divided into four parts. The first one involves water loss (11.8 %) from ambient temperature up to 120 °C. Between 100 and 280 °C the TG curve is flat and no mass loss is detected, and the thermal decomposition (around 65.5 %) occurs after 280 °C, with maxima decomposition temperature at 343 °C, confirmed by DTG curve. Then a continuous carbonization occurs in a wide temperature range from 400 to about 650 °C ($\Delta m = 22.7$ %) [7, 15].

The TG curve of the PM showed the superposition of the thermal behavior of the pure host and guest, indicating multi-step evaporation of the (−)-linalool and the adsorbed water content of β-CD up to 140 °C (Fig. 2). The PM exhibits 18.8 %, and the paste 12.4 % and the slurry 11.9 % of mass loss up to 140 °C (Table 1), respectively. It can be attributed mainly to the water loss and to the release of a small amount of guest from the samples. Between 140 and 280 °C, 1.3–4.6 % further mass change was recorded which may due to the release of the guest compounds from their inclusion complexes (mass loss values are summarized in Table 1). For all studied samples, the main decomposition started above 280 °C indicating the degradation of the inclusion complex and the β-CD (Fig. 2).

Total (−)-linalool retention of the complexes was calculated by subtracting total mass loss, up to 280 °C,

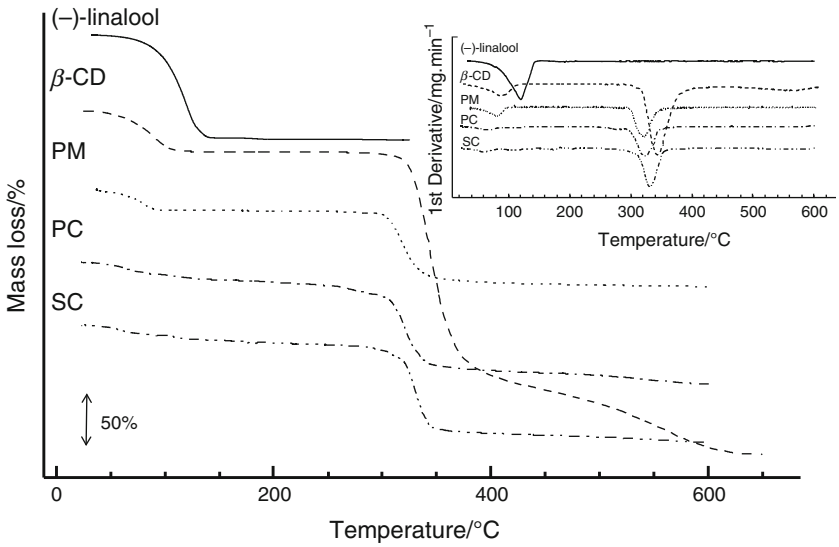

Fig. 2 TG curves of (−)-linalool, β-CD, physical mixture (PM), paste complex (PC) and slurry complex (SC) in dynamic nitrogen atmosphere (50 mL min^{-1}), and hate heat 10 °C min^{-1}

Table 1 Mass losses for (−)-linalool, β-CD, physical mixture, and (−)-linalool-βCD complexes in different temperature intervals ($n = 3$)

Sample	% H_2O (KF)	Δm_1/% 25–140 °C	Δm_2/% 140–280 °C	Δm_3/% 280–400 °C	Δm_4/% 280–400 °C
(−)-Linalol	1.51 ± 0.6	99.2 ± 0.7[a]	–	–	–
β-CD	12.62 ± 0.8	12.2 ± 0.5[b]	0.3 ± 0.5	65.2 ± 0.9[c]	21.4 ± 0.2[d]
Physical mixture (PM)	11.95 ± 0.4	18.8 ± 0.2[e]	1.3 ± 0.1[f]	62.5 ± 0.4[c]	17.1 ± 0.5[d]
Paste complex (PC)	10.99 ± 0.7	12.4 ± 0.9[e]	4.6 ± 0.6[f]	67.6 ± 0.5[c]	14.1 ± 0.7[d]
Slurry complex (SC)	11.48 ± 0.9	11.9 ± 0.8[e]	3.7 ± 0.4[f]	68.7 ± 0.4[c]	14.5 ± 0.5[d]

KF Karl Fischer titration

[a] Percentage of the (−)-linalool evaporates up to 140 °C

[b] Percentage of water releasing up to 140 °C

[c] Thermal decomposition in the interval from 280 to 400 °C

[d] Elemental carbon formation due to sample carbonization in the interval from 400 to 900 °C

[e] Mass loss related to evaporation of the (−)-linalool and the water release up to 140 °C

[f] Mass loss probably attributed to (−)-linalool release in the interval from 140 to 280 °C

from the percentage of water amount determined by the Karl Fisher method, and expressed as a function of the theoretical amount of (−)-linalool added to the complexation medium. It is important to note that TG cannot distinguish between oil and water mass losses from mechanical mixture or inclusion complexes [19]. Thus, a volumetric water determination method (Karl Fisher) was used to estimate total (−)-linalool losses from TG curves. Table 1 lists the percentages of water calculated by the Karl Fisher method.

The thermal behavior of (−)-linalool, β-CD, PM, PC, and SC, previously characterized by TG/DTG analysis, was further investigated by DSC. The DSC curve of (−)-linalool shows an endothermic peak at nearly 140 °C corresponding to its decomposition and volatilization. The DSC curve of β-CD showed a wide endothermic peak at about 82 °C (Fig. 3). The broad endothermic peak was related to dehydration of water molecules that bind to cyclodextrin molecules [20]. In the DSC curve of β-CD (Fig. 3), a small endothermic peak was observed at 225 °C without any mass loss; this represents a physical process and is attributed to the reversible transformation of β-CD [21].

Besides, the base shift around 310 °C may result from a degradation process of β-CD. As can be seen in Fig. 3, the curves corresponding to (−)-linalool/β-CD complexes did not show a sharp endothermic peak in the range of the volatilization of the pure compound (140 °C). The disappearance of this event is due to its encapsulation in the host β-CD (Fig. 3).

Thus, the DSC curves of the (−)-linalool/β-CD complexes indicates endothermic peaks: the first in the range of 25–160 °C (which correspond to the release of water molecules as well as to the release of (−)-linalool, probably adsorbed in the surface), the second in the range of 160–280 °C, where (−)-linalool strong encapsulated is released, and at ∼280 °C, where the decomposition of

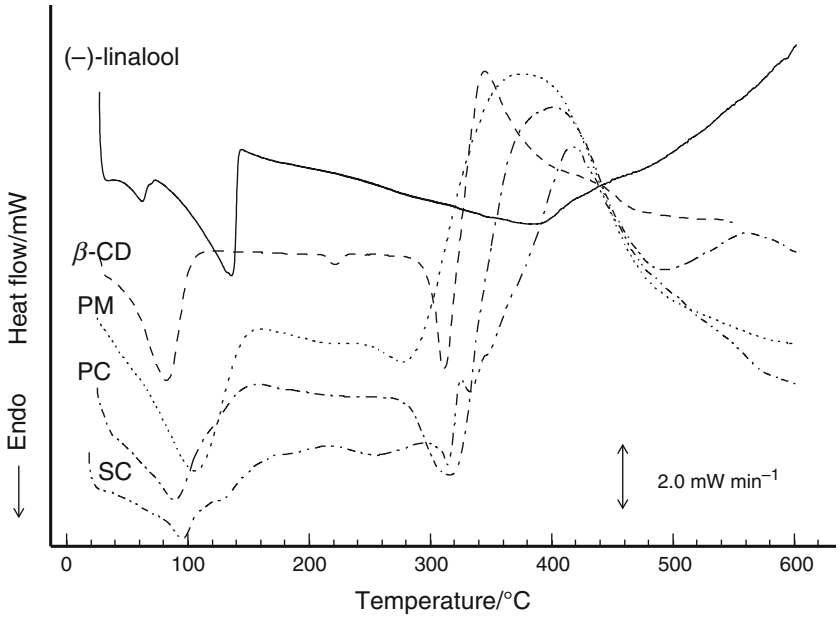

Fig. 3 DSC curves of (−)-linalool, β-CD, physical mixture (PM), paste complex (PC), and slurry complex (SC) in dynamic nitrogen atmosphere (50 mL min^{-1}) and hate heat 10 °C min^{-1}

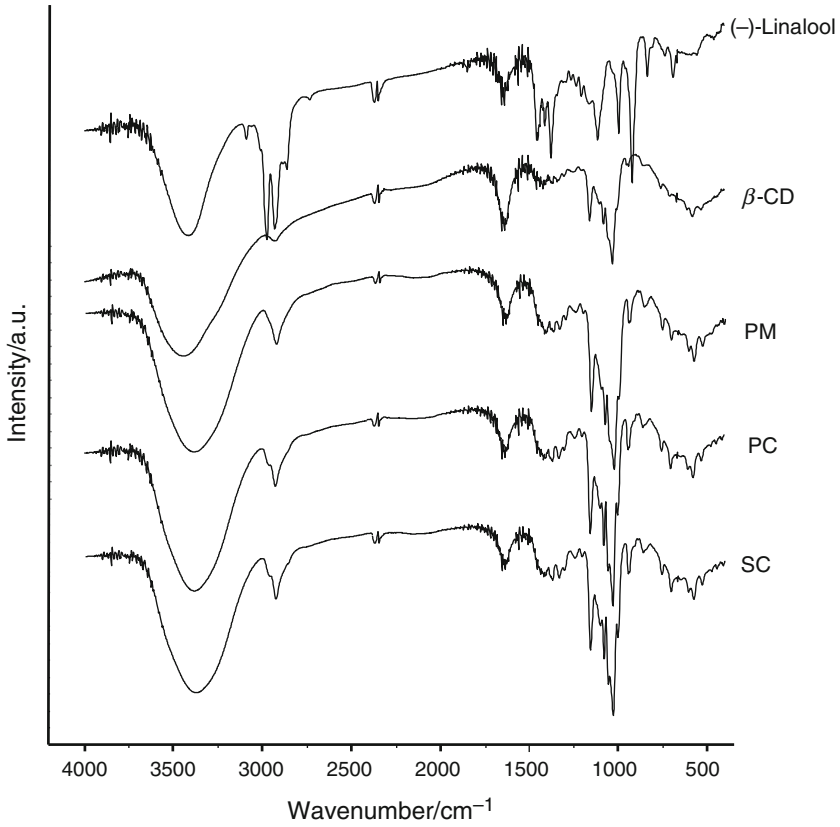

Fig. 4 The infrared spectra of (−)-linalool, β-CD, physical mixture (PM), paste complex (PC), and slurry complex (SC)

cyclodextrin molecules appears. In the case of β-CD, only the peaks corresponding to the release of water molecules (higher than in the case of complexes) and to decomposition appear (Fig. 3). The difference in the DSC curves of the PM and the complexes of (−)-linalool/β-CD clearly indicate complex formation between the components.

FT-IR is a useful technique used to confirm the formation of an inclusion complex. Figure 4 shows IR spectra of (−)-linalool, β-CD, PM, PC, and SC. The FT-IR spectrum of (−)-linalool consisted of the prominent absorption bands at 3,412 cm^{-1} (for O–H stretching vibrations), C–H stretching (2,972 cm^{-1}), C–H aliphatic band appears within the region

2,929 cm^{-1} and C–O stretching band (1,000 cm^{-1}). The very intense peak at 1,644 cm^{-1} is attributed to C=C stretching vibration of the allyl group. The IR spectrum of the pure β-CD (Fig. 4) shows a broad band with an absorption maximum centered at about 3,340 cm^{-1}, due to the O–H stretching vibrations of the different hydroxyl groups of the β-CD. A band at 1,647 cm^{-1}, related to the bending vibrations of these OH groups, is also well visible. The spectrum presents several other bands, mainly at 2,926 cm^{-1} (C–H stretching vibrations of the CH and CH_2 groups), at 1,411, 1,368, 1,335, 1,301, and 1,246 cm^{-1} due to C–H bending vibrations, and at 1,154, 1,080, and 1,027 cm^{-1} attributed to the C–O stretching vibrations of the bonds in the ether and hydroxyl groups. Finally typical bands in the region 1,000–700 cm^{-1}, belonging to the rocking vibrations of the C–H bonds and the C–C skeletal vibrations in the glucopyranose ring, are also present. Similar results were obtained by Scirè et al. [22].

The peak at 1,000 cm^{-1}, of the C–O group, was the most important characteristic of the (−)-linalool. The intensity of band was used as an internal reference for the content in the β-CD complexes. In all spectra, this band

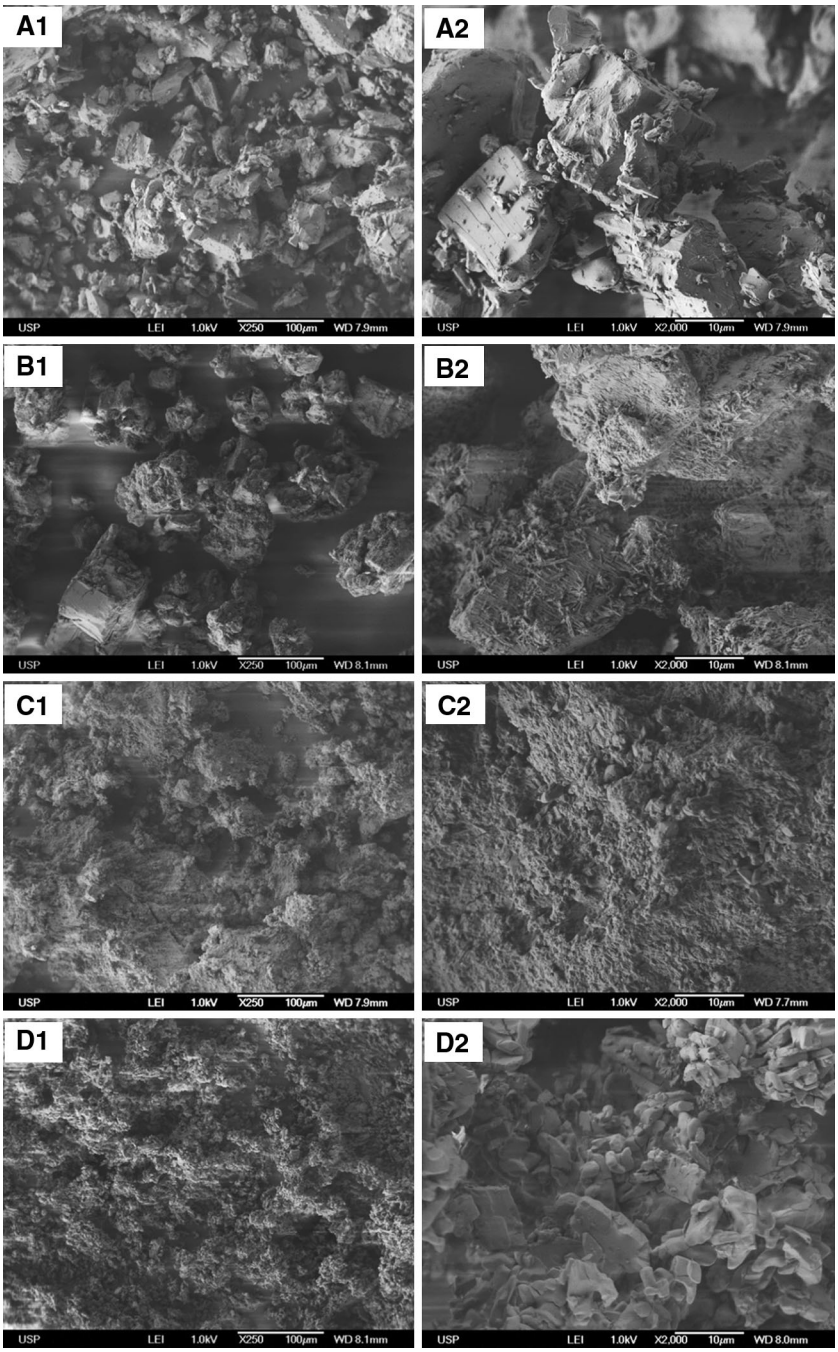

Fig. 5 SEM micrographs of cross-sections (1 and 10 μm, 1 and 2, respectively) of **a** β-CD, **b** physical mixture (PM), **c** paste complex (PC) and **d** slurry complex (SC)

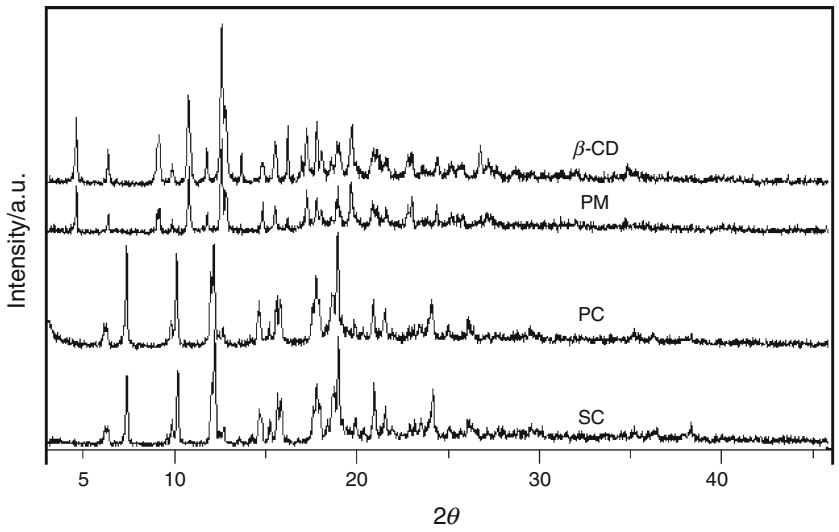

Fig. 6 X-ray diffraction of **a** β-CD, **b** physical mixture (PM), **c** paste complex (PC), and **d** slurry complex (SC)

Table 2 Characterization of complexes of inclusion by gas chromatography/mass spectrometry (GC/GCMS) analyses

Sample	Extracts		Conc. % difference of extracts from original linalool	
	Surface linalool	Total lilinalool	Compl. linalool/%	Complexation ratio
Physical mixture	98.23	1.89	−90.77	None
Paste complex	61.52	70.12	8.6	1:8.6
Slurry complex	42.41	84.98	42.57	1:1

presented a small shift due to the formation of hydrogen bonds between the molecule of (−)-linalool and the molecule of β-CD. In addition, the relative intensities of SC and PC are different.

Figure 5 shows the SEM images of β-CD, PM, PC, and SC powders at different magnifications. The β-CD was composed of different sizes of rectangular-shaped crystals. In addition, there were small particles that adhered to the surfaces of the crystals, which is in agreement with the observations made by other authors [23–26]. As seen from Fig. 5, there were drastic changes in particle shapes and original morphologies of the inclusion complex products. The complexation between (−)-linalool and β-CD appeared as agglomerates. In contrast, the particle shapes and morphologies of the corresponding PMs were similar to those of β-CD. The particle sizes of the PMs were much larger than those of the inclusion complex products. A very interesting paper is by Haiyee et al. [27]. In this paper, the authors studied the inclusion complexes of turmeric oleoresin and cyclodextrin. Haiyee et al. reported that in the co-precipitation samples, the original morphology of the raw materials disappeared, and it was not possible to differentiate the final products from the starting materials. The drastic change of the particles' shapes and aspects in the co-precipitation sample were indicative of the presence of a new solid phase. This result was corroborated by XRD which showed that different crystal structures for the products were obtained by slurry and paste methods.

The XRD profiles of the β-CD, PM, PC, and SC are shown in Fig. 6. The upper one is belonging to the crystalline β-CD, itself [28, 29]. It was observed that inclusion complex formation induced large shifts in the wide angle XRD signals of β-CD. Furthermore, the SC and PC had different XRD signals compared with PM and β-CD. The binary mixtures showed several peaks attributable to crystalline β-CD. Only a slight decrease in peak intensity was noted. In comparison, the complexes of (−)-linalool/β-CD obtained by kneading method and paste showed the disappearance of reflections and the appearance of new peaks. No inclusion complex was obtained by PMs, while PC and SC products showed weak interactions confirming the DSC and TG/DTG results. These results clearly demonstrated the formation of inclusion complex between (−)-linalool and β-CD. Kedzierewicz et al. and Byun and Whiteside [30, 31] reported similar findings for tolbutamide/β-cyclodextrin complex and ascorbyl palmitate/β-CD system, respectively. According to Pedersen et al. [32] in the study of econazole/β-CD complex, distinct lines on an X-ray powder diffraction spectrum, i.e., the complex is crystalline although it is difficult to recognize the crystalline structure of this complex.

Data analysis by GC–MS/FID of the (−)-linalool total and surface-adsorbed determined the amount of linalool present in

the β-CD cavity and inclusion relation to each procedure complexation (Table 2). Thus, the subtraction of the total (−)-linalool from the surface-adsorbed linalool correspond to the amount complexed in the β-CD cavity. Menthol was used as internal standard. PC procedure showed 8.6 % of (−)-linalool in complex cavity. On the other hand, SC showed 42.57 % of (−)-linalool in complex cavity, which conduces to a more efficient complexation of (−)-linalool. PM procedure showed no significant results. Bhandari et al. reported that lemon oil can be successfully produced according to the paste or kneading method using β-CD [33]. Study performed by Numanoğlu et al. [34] demonstrated that inclusion complexes of linalool with 2-HPβCD present significantly increase of the water solubility of this compound. The controlled release of linalool can be achieved by preparing inclusion complexes, and the stability of these compounds in the gel formulations can be increased by complexation. So, the formation of the inclusion complex containing β-cyclodextrin (β-CD) and (−)-linalool has shown promise for pharmacological use with prospects for future clinical approach [35].

Conclusions

This study was concerned with the preparation of an inclusion complex of (−)-linalool with β-CD, and subsequent analysis of the complex using various analytical techniques for their comparison. The combined use of different characterization techniques has provided practical evidence for the formation of complexes. The results of this study clearly demonstrated that (−)-linalool could be successfully produced according to the paste or slurry method.

Acknowledgements We would like to thank the Conselho Nacional de Desenvolvimento Científico e Tecnológico/CNPq/Brazil) and Fundação de Amparo à Pesquisa do Estado de Sergipe/FAPITEC-SE for the financial support.

References

1. Venâncio AM, Marchioro M, Estavam CS, Melo MS, Santana MT, Onofre ASC, Guimarães AG, Oliveira MGB, Alves PB, Pimentel HC, Quintans-Júnior LJ. *Ocimum basilicum* (Lamiaceae) leaf essential oil and (−)-linalool reduce orofacial nociception in rodents—a behavioral and electrophysiological approach. Braz J Pharmacogn. 2011;21:1043–51.
2. Letizia CS, Cocchiara J, Lalko J, Api AM. Fragrance material review on linalool. Food Chem Toxicol. 2003;41:943–64.
3. Kamatou GPP, Viljoen AM. Linalool—a review of a biologically active compound of commercial importance. Natural Prod Commun. 2008;3(7):1183–92.
4. Peana AT, D'Aquila PS, Panin F, Serra G, Pippia P, Moretti MDL. Antiinflammatory activity of linalool and linalyl acetate constituents of essential oils. Phytomedicine. 2002;9:721–6.
5. Peana AT, D'Aquila PS, Chessa ML, Moretti MDL, Serra G, Pippia P. (−)-Linalool produces antinociception in two experimental models of pain. Eur J Pharmacol. 2003;460:37–41.
6. Marreto RN, Almeida EECV, Alves PB, Niculau ES, Nunes RS, Matos CRS, Araújo AAS. Thermal analysis and gas chromatography coupled mass spectrometry analyses of hydroxypropyl-β-cyclodextrin inclusion complex containing *Lippia gracilis* essential oil. Thermochim Acta. 2008;475:53–8.
7. Astray G, Gonzalez-Barreiro C, Mejuto JC, Rial-Otero R, Simal-Gándara J. A review on the use of cyclodextrins in foods. Food Hydrocoll. 2009;23(7):1631–40.
8. Zhang J, Ma PX. Cyclodextrin-based supramolecular systems for drug delivery: recent progress and future perspective. Adv Drug Deliv Rev 2013. doi:10.1016/j.addr.2013.05.001.
9. Uekama K, Hirayama F, Irie T. Cyclodextrin drug carrier systems. Chem Rev. 1998;98(5):2045–76.
10. Serafini MR, Menezes PP, Costa LP, Lima CM, Quintans LJ Jr, Cardoso JC, Matos JR, Soares-Sobrinho JL, Grangeiro S Jr, Nunes PS, Bonjadim LR, Araújo AAS. Interaction of p-cymene with β-cyclodextrin. J Thermal Anal Calorim. 2012;109:951–5.
11. Ghosh I, Nau WM. The strategic use of supramolecular pK_a shifts to enhance the bioavailability of drugs. Adv Drug Deliv Rev. 2012;64(9):764–83.
12. Li J, Loh XJ. Cyclodextrin-based supramolecular architectures: syntheses, structures, and applications for drug and gene delivery. Adv Drug Deliv Rev. 2008;60:1000–17.
13. Cevallos PAP, Buera MP, Elizalde BE. Encapsulation of cinnamon and thyme essential oils components (cinnamaldehyde and thymol) in β-cyclodextrin: effect of interactions with water on complex stability. J Food Eng. 2010;99:70–5.
14. Del Valle M. Cyclodextrins and their uses: a review. Process Biochem. 2004;39:1033–46.
15. Xu P, Song LX, Wang HM. Study on thermal decomposition behavior of survived β-cyclodextrin in its inclusion complex of clove oil by nonisothermal thermogravimetry and gas chromatography coupled to time-of-flight mass spectrometry analyses. Thermochim Acta. 2008;469:36–42.
16. Menezes PP, Serafini MR, Santana BV, Nunes RS, Quintans LJ Jr, Silva GF, Medeiros IA, Marchioro M, Fraga BP, Santos MRV, Araújo AAS. Solid-state β-cyclodextrin complexes containing geraniol. Thermochim Acta. 2012;548:45–50.
17. Ciobanu A, Mallard I, Landy D, Brabie G, Nistor D, Fourmentin S. Inclusion interactions of cyclodextrins and crosslinked cyclodextrin polymers with linalool and camphor in *Lavandula angustifolia* essential oil. Carbohydr Polym. 2012;87:1963–70.
18. The American Society for testing and materials. Philadelphia: Annual Book of ASTM Standards 14; 1993. p. 1582.
19. Hădărugă DI, Hădărugă NG, Bandur GN, Isengard H-D. Water content of flavonoid/cyclodextrin nanoparticles: relationship with the structural descriptors of biologically active compounds. Food Chem. 2012;132:1651–9.
20. Scirè S, Giuffrida S, Crisafulli C, Riccobene PM, Pistone A. Liquid phase photo-deposition in the presence of unmodified β-cyclodextrin: a new approach for the preparation of supported Pd catalysts. J Mol Catal A. 2012;353–354:87–94.
21. Guo P, Su Y, Cheng Q, Pan Q, Li H. Crystal structure determination of the β-cyclodextrin–p-aminobenzoic acid inclusion complex from powder X-ray diffraction data. Carbohydr Res. 2011;346:986–90.
22. Wang J, Cao Y, Sun B, Wang C. Physicochemical and release characterization of garlic oil-β-cyclodextrin inclusion complexes. Food Chem. 2011;127:1680–5.
23. Songkro S, Hayook N, Jaisawang J, Maneenuan D, Chuchome T, Kaewnopparat N. Investigation of inclusion complexes of citronella oil, citronellal and citronellol with β-cyclodextrin for mosquito repellent. J Incl Phenom Macrocycl Chem. 2012;72:339–55.

24. Fujiwara T, Yamazaki M, Tomizu Y, Tokuoka R, Tomita K, Matsuo T. The crystal structure of a new form of β-cyclodextrin water inclusion compound and thermal properties of β-cyclodextrin inclusion complexes. Nippon Kagaku Kaishi. 1983;181:187.
25. Santos C, Buera MP, Mazzobre MF. Influence of ligand structure and water interactions on the physical properties of β-cyclodextrins complexes. Food Chem. 2012;132:2030–6.
26. Hădărugă NG. *Ficaria verna* Huds. extracts and their β-cyclodextrin supramolecular systems. Chem Cent J. 2012;6:16.
27. Haiyee ZA, Saim N, Said M, RMd Illias, Mustapha WAW, Hassan O. Characterization of cyclodextrin complexes with turmeric oleoresin. Food Chem. 2009;114:459–65.
28. Martins AP, Craveiro AA, Machado MIL, Raffin FN, Moura TF, Novák Cs, Éhen Z. Preparation and characterization of mentha x villosa Hudson oil-β-cyclodextrin complex. J Thermal Anal Calorim. 2007;88(2):363–71.
29. Zingone G, Rubessa F. Preformulation study of the inclusion complex warfarin-β-cyclodextrin. Int J Pharm. 2005;291:3–10.
30. Kedzierewicz F, Hoffman M, Maincent P. Comparison of tolbutamide/β-cyclodextrin inclusion and solid dispersions compounds: physicochemical characteristics and dissolution studies. Int J Pharm. 1990;58:221.
31. Byun Y, Whiteside S. Ascorbyl palmitate-β-cyclodextrin inclusion complex as an oxygen scavenging microparticle. Carbohydr Polym. 2012;87:2114–9.
32. Pedersen M, Bjerregaard S, Jacobsen J, Larsen AR, SØrensen AM. An econazole-cyclodextrin inclusion complex: an unusual dissolution rate, supersaturation, and biological efficacy example. Int J Pharm. 1998;165:57–68.
33. Bhandari BR, D'Arcy BR, Padukka I. Encapsulation of lemon oil by paste method using β-cyclodextrin: encapsulation efficiency and profile of oil volatiles. J Agric Food Chem. 1999;47:5194–7.
34. Numanoğlu U, Şen T, Tarimci N, Kartal M, Koo OMY, Onyuksel H. Use of cyclodextrins as a cosmetic delivery system for fragrance materials: linalool and benzyl acetate. AAPS PharmSciTech. 2007;8(4):E85.
35. Quintans-Júnior LJ, Barreto RS, Menezes PP, Almeida JR, Viana AF, Oliveira RC, Oliveira AP, Gelain DP, de Lucca Júnior W, Araújo AAS. β-Cyclodextrin-complexed (−)-linalool produces antinociceptive effect superior to that of (−)-linalool in experimental pain protocols. Basic Clin Pharmacol Toxicol. 2013;113(3):167–72.